Dielectric and IR Spectroscopy of the Macromolecular Reaction of Anhydridization in a Functionalized Side-Chain Liquid Crystalline Copolymer Containing Acrylic Acid Groups

ARTICLE *in* MACROMOLECULES · MAY 2001

Impact Factor: 5.8 · DOI: 10.1021/ma0018401

8 AUTHORS, INCLUDING:

Sergey Zhukov
Technical University Darmstadt
34 PUBLICATIONS **265** CITATIONS
SEE PROFILE

E.B. Barmatov
Schlumberger Limited
114 PUBLICATIONS **580** CITATIONS
SEE PROFILE

Valery Petrovich Shibaev
Lomonosov Moscow State University
411 PUBLICATIONS **4,695** CITATIONS
SEE PROFILE

Friedrich Kremer
University of Leipzig
302 PUBLICATIONS **6,182** CITATIONS
SEE PROFILE

Dielectric and IR Spectroscopy of the Macromolecular Reaction of Anhydridization in a Functionalized Side-Chain Liquid Crystalline Copolymer Containing Acrylic Acid Groups

Sergei Zhukov and Bernd Stühn*

Technische Universitat Ilmenau, Institut für Physik, 98693 Ilmenau, Germany

Tamara Borisova

Institute of Macromolecular Compounds of Russian Academy of Sciences, 199004 St. Petersburg, Russia

Evgenii Barmatov, Marina Barmatova, and Valery Shibaev

Chemistry Department, Moscow State University, 119899, Moscow, Russia

Friedrich Kremer

Leipzig University, Faculty of Physics and Geosciences, 504103 Leipzig, Germany

Polycarpos Pissis

Department of Physics, National Technical University of Athens, 15780 Athens, Greece

Received October 26, 2000; Revised Manuscript Received February 27, 2001

ABSTRACT: The anhydrization reaction has been investigated in functionalized side-chain random liquid crystalline (LC) copolymers containing cyanobiphenyl mesogenic and acrylic acid (38 mol %) groups. Heat treatment of the LC copolymer at 130 °C for 5−200 h is accompanied by formation of intra- and intermolecular anhydrides and network structures causing an increase of the glass transition and clearing temperatures. The influence of annealing on the reorientational dynamics of the copolymers was investigated by broad-band dielectric relaxation spectroscopy. The local dynamics of the side group involving spacer motion (γ relaxation) and mesogen rotation about the long axis (β relaxation) do not depend on the annealing time. At the same time a considerable (more than 2 orders of magnitude) decrease in the relaxation rates of the cooperative δ and α processes was observed due to a gradual increase in the main-chain rigidity during the annealing. The molecular mechanism of all relaxation processes detected is discussed.

1. Introduction

An approach to the preparation of a new class of polymer liquid crystalline materials, the so-called functionalized LC polymers, has been proposed.[1−13] These compounds are random copolymers of two monomers. One of the monomers is mesogenic and favors LC phase formation. The other monomer is functional and contains carboxylic groups (acrylic,[5−7] maleic,[8] benzoic acids[1,2,9−13]) capable of forming hydrogen bonds. The presence of carboxylic groups in the functionalized LC polymers offers the possibility to control the properties of the macromolecules simply by changing the ratio of acid to mesogenic fragments.

It is well-known[14] that in poly(acrylic acid) and its copolymers reactions of intramolecular transformation take place at temperatures between 130 and 250 °C. The products of these reactions are water (dehydration or anhydrization reaction) and carbon dioxide (decarboxylation reaction). At temperatures up to 170 °C, the reaction proceeds mainly with water elimination and anhydride group formation. Depending on the character of the macromolecular reaction, both intra- and intermolecular anhydride structures can be formed. It should be noted that the configurational composition and the packing defects of the polymer chain essentially determine the character of the products of the anhydrization. Thus, it has been shown[14] that in poly(acrylic acid) and its polycomplexes intermolecular anhydrides are mostly formed in defective regions (folds and overlapping), whereas intramolecular anhydrides are formed in ordered regions of the polymer chain packing.

The present work deals with the formation of anhydride structures in a side-chain functionalized LC copolymer **P1** containing acrylic acid groups:

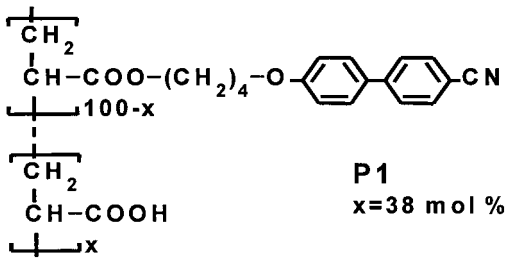

P1
x=38 mol %

The study of dehydration in a functionalized LC copolymer had the following aims. First, the investigation of the anhydrization process itself as well as establishment of the character of the resulting anhydride structures. In the case of intramolecular water elimination, intramolecular anhydride rings are formed. The intermolecular dehydration leads to formation of anhydride cross-links and a network structure. Second, it was important to determine the effect of the anhy-

10.1021/ma0018401 CCC: $20.00
Published on Web 04/27/2001

dride structures on the ability of mesogenic groups to form LC state as well as to investigate the dynamics of the relaxation processes. At present, very few publications studying the anhydrization in the functionalized side-chain LC polymers are available.[5−8]

In the present work FTIR and dielectric spectroscopy were used as principal investigation methods. They allow studying of both the character of the molecular transformations of the acid fragment of the functionalized LC copolymer and the effect of the anhydride structures on processes related to the molecular mobility and the relaxation of the mesogenic groups in the different phase states of the system (the glassy state, the LC phase, and the isotropic melt).

2. Experimental Section

2.1. Synthesis of the Functionalized LC Copolymers. The monomer 4-(4-cyanobiphenyl-4′-yloxy)butyl acrylate (**CB**) was prepared by common synthetic procedures. The copolymer **P1** was obtained by a free-radical copolymerization of monomers **CB** and acrylic acid in absolute THF at 65 °C; AIBN (2 wt %) was used as initiating agent. The so-synthesized copolymers were purified by repeated precipitation from THF solutions by hexane. The composition of the copolymer was determined by elemental analysis.

CB (K 93 °C I). ^{1}H NMR ($CDCl_3$): δ 7.97 (d, 2H, Ph, J = 8.85 Hz); 7.67 (d, 2H, Ph, J = 8.55 Hz); 7.62 (d, 2H, Ph, J = 8.51 Hz); 7.51 (d, 2H, Ph, J = 8.81 Hz); 6.35 (dd, 1H, CH_2═CH−, J = 1.65; 17.65 Hz); 6.12 (dd, 1H, CH_2═CH−, J = 10.3; 17.31 Hz); 5.81 (dd, 1H, CH_2═CH−, J = 1.65; 10.3 Hz); 4.21 (t, 2H, O−CH_2); 4.02 (t, 2H, −CH_2−O); 1.89 (4H, −CH_2−CH_2−).

2.2. Characterization. Microcalorimetric studies were performed with a "Mettler" differential scanning calorimeter TA4000. The heating rate was 10 K/min. Polarizing optical microscopy observations were made with a Zeiss polarizing microscope equipped with a Mettler FP-82HT hot stage controlled by a Mettler FP90 unit. X-ray diffraction analysis was carried out using an URS-55 instrument (Ni-filtered Cu Kα radiation).

2.3. Fourier Transform Infrared Spectroscopy (FTIR). The FT spectra were recorded by a FTIR spectrometer (Biorad FTS 6000) in the region 600−4000 cm^{-1} at a spectral resolution of 4 cm^{-1} and an uncertainty < 5% in absorbance. A standard GRAMS program was used for the separation of the overlapping bands. For the absorbance measurements the sample was confined between two KBr windows. This preparation procedure results in a film thickness of 5−8 μm, which corresponds to a maximum absorbance of approximately 0.7−1.0.

2.4. Molar Mass Determination. The relative molecular weights of the polymers were determined by gel permeation chromatography (GPC) using a GPC-2 Waters instrument equipped with a LC-100 column oven and a Data Modul-370 data station. The measurements were done using an UV detector, THF as solvent (1 mL/min, 25 °C), a set of PL columns of 100, 500, and 10^3 Å, and a calibration plot constructed with polystyrene standards.

2.5. Dielectric Spectroscopy (DS). Dielectric experiments in the frequency range 10^{-2}−10^8 Hz were carried out by measuring the complex impedance with two different setups. In the range 10^{-2}−10^6 Hz we used the Solartron−Schlumberger frequency response analyzer SI1260 equipped with a Chelsea dielectric interface. In the range 10^6−10^8 Hz, a rf impedance analyzer (HP 4191A) was employed. The sample capacitor consisting of two gold-coated stainless steel electrodes was filled with the polymer at temperatures above the clearing temperature. A constant sample thickness of 105 ± 1 μm was maintained by use of silica spacers. Polymer **P1** was subjected to anhydrization directly in the capacitor at 130 ± 1 °C for 50, 100, 150, or 200 h. The same capacitor was used for sample preparation with different thermal treatment times. This procedure ensured the identity of the empty capacity (C_0) of the dielectric cell for all DS measurements. Prior to each frequency scan, the sample was thermally equilibrated at the selected temperature with a stability better than 0.2 °C. All samples were measured in an unaligned state.

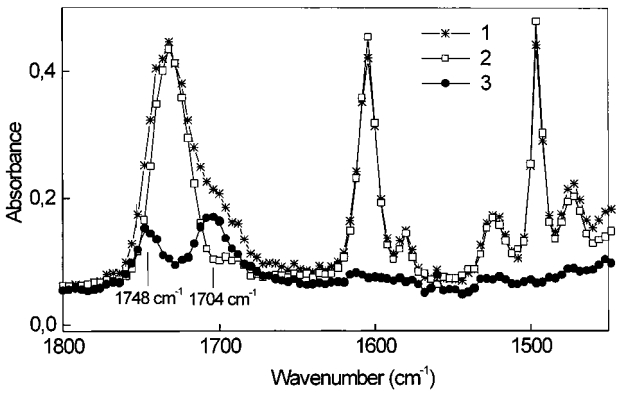

Figure 1. Infrared spectra at 60 °C for the copolymer **P1** (1), the homopolymer **pCB** (2), and the differential spectrum **P1** − **pCB** (3).

3. Results and Discussion

3.1. Influence of the Annealing Time on the Phase Transitions and Structure of the Functionalized LC Copolymer P1. A random LC copolymer containing 38 mol % of acrylic acid groups was used for anhydrization studies. Molecular weight M_w and molecular weight distribution (M_w/M_n) are 4600 and 1.2, respectively. The degree of polymerization of this polymer is 41, and its phase behavior is characterized by the sequences *glass 42 SmA 97 I*.[15]

The phase state of the LC copolymer **P1** was investigated by polarizing microscopy, DSC, and X-ray diffraction. The SmA phase forms a fine grain texture. The X-ray diffraction patterns of the SmA phase after orientation by mechanical shift exhibit small (d_1 = 33.9 Å, d_2 = 17.1 Å) and wide-angle reflections (D = 4.9 Å) split in mutually perpendicular directions. The DSC curves show a single endothermic peak with the heat of melting ΔH = 1.1 J/g. The parameters of the layer packing in the SmA phase of **P1** copolymer do not depend on the time of the thermal treatment.

Figure 1 (curve 1) shows the IR spectrum of the copolymer **P1**. In the range 1650−1750 cm^{-1} it exhibits a series of overlapping bands due to carbonyl stretching vibrations [$\nu_{C=O}$] in ester and carboxylic groups. Differential spectra obtained by subtracting the IR spectrum of the homopolymer **pCB** (curve 2) from that of the **P1** copolymer were studied. The normalization was carried out from ∼1600 to ∼1500 cm^{-1} bands of the benzene rings oscillations. This procedure allows to subtract the absorption of the ester fragments in the mesogenic groups from the copolymer spectrum. Hence, only the vibration bands of the acid groups are present in the normalized spectrum (curve 3). The differential IR spectrum exhibits two bands [$\nu_{C=O}$], at 1748 and 1704 cm^{-1}, which are assigned to the free and bonded by hydrogen bonds carboxylic groups, respectively.

We conclude that intramolecular hydrogen bonds are formed in the investigated LC copolymer **P1**. They are schematically shown in Figure 2a. According to our previous investigations,[5−7] intramolecular eight-membered alicyclic rings determine the phase state of the LC polymer **P1**. The mechanism of this effect consists of the restriction of the rotational freedom of the

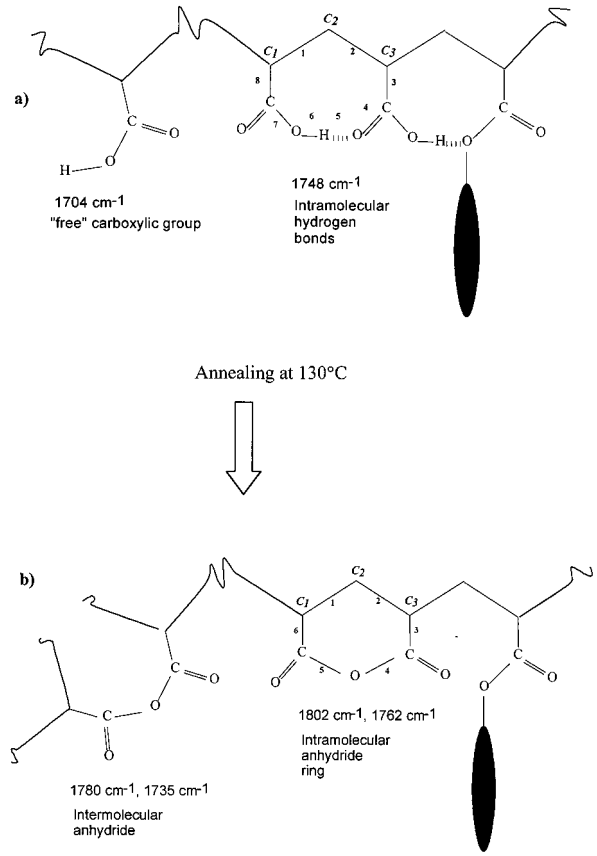

Figure 2. Schematic diagram illustrating the part of the polymer chain of the copolymer **P1** before (a) and after (b) annealing.

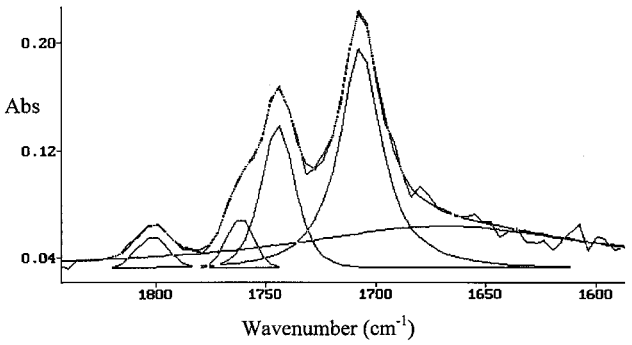

Figure 3. Differential infrared spectrum in the carbonyl stretching region obtained by subtracting curve 2 (Figure 1) from the spectrum of the copolymer **P1-8**. Curve-fitting results of the annealing samples are collected in Table 1.

monomer units by the hydrogen bonds. The restriction of the internal rotation to the limits of the arc angle leads to increasing rigidity of the polymer chain.

The functionalized LC copolymer **P1** was annealed at 130 °C for 5−200 h. Figure 3 shows differential IR spectra of this copolymer after annealing at 130 °C for 8 h. It is clear that in the region of stretching vibrations [$\nu_{C=O}$] the two additional bands, at 1802 and at 1762 cm^{-1}, appear as a result of contour separation. They are assigned to stretching vibrations of the carbonyl group in the six-membered ring. With increasing the annealing time (Table 1), a decrease of the bands of the carboxylic groups (1748 and 1704 cm^{-1}) and an increase of the intensity of the bands at 1802 and 1762 cm^{-1} are observed. This indicates that the fraction of the intramolecular anhydride rings increases. The ratio of the

Table 1. Influence of the Annealing Time on the Intensity of the Carbonyl Bond [$\nu_{C=O}$]

annealing time, h	D_{1762}/D_{1748}	D_{1762}/D_{1703}
8	0.37 ± 0.02	0.23 ± 0.02
26	0.51 ± 0.03	0.32 ± 0.02
50	0.62 ± 0.03	0.39 ± 0.02
100	0.76 ± 0.03	0.57 ± 0.03
150	0.84 ± 0.04	0.62 ± 0.03
200	0.86 ± 0.04	0.64 ± 0.03

Table 2. Influence of the Annealing Time on the Phase Transitions and the Solubility in THF of the Copolymer P1

sample	annealing time, h	phase transition, °C	solubility in THF
P1	0	glass 42 SmA 97 I	dissolved
P1-50	50	glass 58 SmA 105 I	dissolved
P1-100	100	glass 60 SmA 107 I	dissolved
P1-150	150	glass 62 SmA 108 I	nondissolved
P1-200	200	glass 64 SmA 110 I	nondissolved

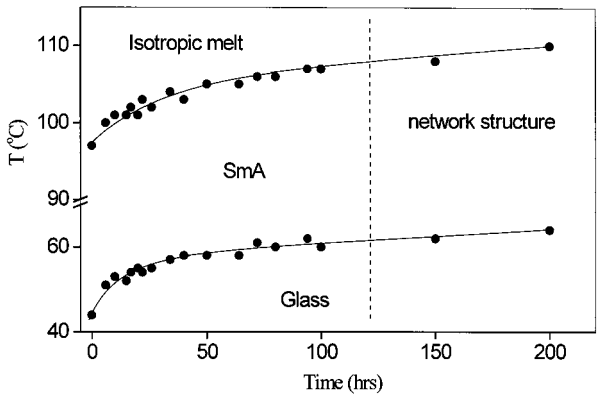

Figure 4. Glass transition and clearing temperatures of the copolymer **P1** vs the annealing time at 130 °C. The line is a guide for the eye.

bands of bound to free COOH groups remains virtually unchanged during the heat treatment.

Figure 4 shows the dependence of the transition temperatures determined by DSC on the annealing time. The same results are also collected in Table 2. It can be seen that the annealing leads to a considerable increase in the clearing and the glass transition temperatures. The region of the most rapid rise of these temperatures is located at annealing times up to 50 h. Further increase in the thermal treatment leads to slower rise of the glass transition temperature and of the melting point. The reason for increasing the transition temperatures is related to macromolecular reactions: water elimination and formation of six-membered rings. Rigid ring formation results in decreasing kinetic flexibility of the polymer chain. It should be noted that the formation of "true" rings exerts greater effect on the chain rigidity than the formation of intramolecular hydrogen bonds only.[5−7]

The samples subjected to long-term annealing at 130 °C for 5−100 h completely retain solubility in THF (see Table 2). The absence of insoluble cross-linked products indicates that mainly intramolecular anhydride rings are formed, which is also confirmed by IR spectroscopy. However, annealing is also accompanied by the formation of intermolecular anhydride bonds (Figure 2b), which leads to increasing the molecular weight of the copolymers. Figure 5 shows data of gel permeation chromatography for the LC copolymers before (curve 1) and after (curves 2 and 3) annealing. The data clearly

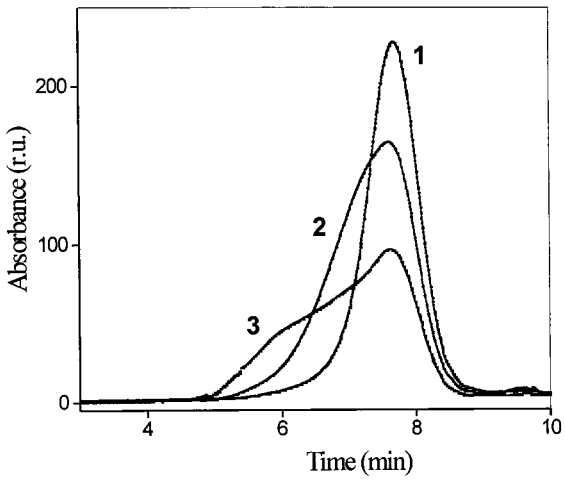

Figure 5. GPC curves for the LC copolymer **P1** before (1) and after annealing at 130 °C for 50 (2) and 100 h (3). The concentration of the polymer sample in the solution is 10 mg/dL.

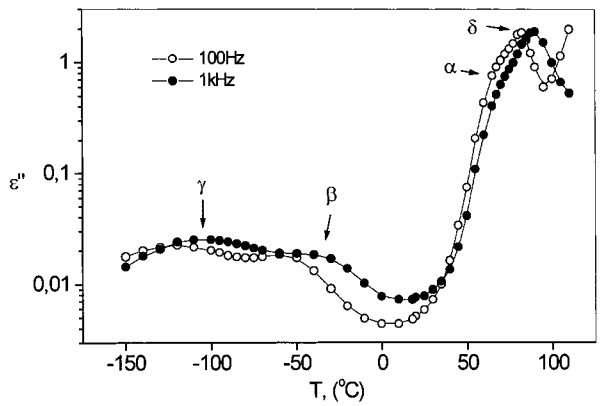

Figure 6. Temperature dependence of the dielectric loss factor ϵ'' at fixed frequencies for the copolymer **P1**.

show that the thermal treatment for 50−100 h leads to the appearance of a high molecular weight shoulder on the GPC curve. This indicates that the molecular weight and the polydispersity of the copolymer **P1** increase. For an annealing time of 5−40 h, no visible broadening of GPC curves was observed. Unfortunately, due to low concentration of the intermolecular anhydride groups and to strong band overlapping, the IR spectroscopy could not single out characteristic bands at 1780 and at 1735 cm^{-1} for the saturated acyclic anhydride.

The samples **P1-150** and **P1-200** do not dissolve but swell considerably in THF. This means that a cross-linked structure has formed in the samples annealed for 150 or 200 h. Hence, the following conclusion may be drawn. The heat treatment of functionalized LC polymers for 5−200 h leads to the formation of the following series of macromolecular products: (i) six-membered intramolecular anhydride rings; (ii) intermolecular anhydride; (iii) network structure. It is reasonable to suggest that each of the above structures provides a different contribution to the thermostability of the functionalized LC polymer **P1**.

The formation of six-membered intramolecular rings gives the greatest contribution to the increase in the mesophase thermal stability. This is reflected in a strong rise of the transition temperatures at the initial annealing stage (up to 50 h). However, the formation of the six-membered rings is limited by the fact that only neighboring carboxylic groups of the acrylic acid can participate in this reaction. The quantity of these fragments is limited by the relatively low acrylic acid content and by the random distribution of the monomer units in the polymer **P1**. Therefore, when the reaction in the acrylic acid groups with microblock distribution completes, isolated acrylic acid units begin to take part in the reaction of anhydridization.

Isolated acrylic acid groups can form only intermolecular anhydride structures, leading to increasing the molecular weight and the branching of the polymer **P1**. This process is completed by the formation of a three-dimensional network structure. According to the literature data,[16] maximum rise in the transition temperatures of side-chain LC polymers with increasing molecular weight is observed at degree of polymerization (DP) up to 60−80. At high DP values, polymer properties are virtually independent of the chain length. The investigated LC polymer **P1** has DP = 41. Hence, a great increase in the clearing temperature by 13 °C and in the glass transition temperature by 22 °C cannot be due to increasing the molecular weight of the polymer **P1**. This point is also valid for the effect of the network structure on the phase behavior of the polymers. A considerable change of the glass transition temperatures in the networks is possible only at high cross-linking density. The network structure formation in the polymer **P1** starts at annealing times longer than 100 h. However, the maximum increase in the transition temperature is observed in the range from 5 to 50 h (i.e., under these conditions the network is not formed at all). Consequently, the main reason for changes in the phase behavior of the investigated LC polymer **P1** is the formation of a ladderlike structure (intramolecular six-membered rings). The contribution of the intermolecular anhydrides and the cross-linked structure to the increase in the transition temperatures is much smaller.

At the end of this section we will consider the problem of the characterization of the cross-linked LC polymers **P1-150** and **P1-200** (see Table 2). According to the results of an investigation in dilute solution, the polymer chain of the functionalized LC polymer **P1** is a rodlike particle.[15] At an average degree of polymerization DP = 41, the **P1** macromolecule consists of approximately three to four random Kuhn segments. Hence, in analyzing the parameters of the network structure (the average molecular weight of the chain segment between cross-links or the junction functionality), we cannot use methods based on statistical gel formation theory. The initial polymer **P1** used for network formation is only an oligomer. Therefore, its behavior cannot be described by the Flory statistics. Moreover, even at a cross-linking density of three, the distance between two junctions becomes shorter than the random segment length. At the same time it is well-known that the application of the methods based on the concepts of an ideal polymer network for analysis of high-density networks is very problematic and has no unique solution.

The effect of the anhydride and the network structures on the dynamic behavior of the functionalized LC copolymer will be considered in the next sections dealing with broad-band dielectric spectroscopy.

3.2. Dielectric Spectroscopy of the Macromolecular Reaction of Anhydridization in the Functionalized LC Copolymer P1. 3.2.1. Functionalized LC Copolymer P1. Figure 6 shows the temperature dependence of the dielectric loss factor at two frequencies for the functionalized LC polymer **P1**. It can

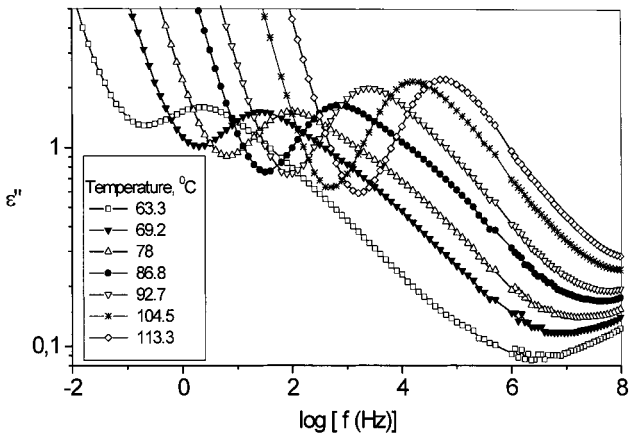

Figure 7. Dielectric loss factor ϵ'' vs frequency for the copolymer **P1** at different temperatures (LC and isotropic states).

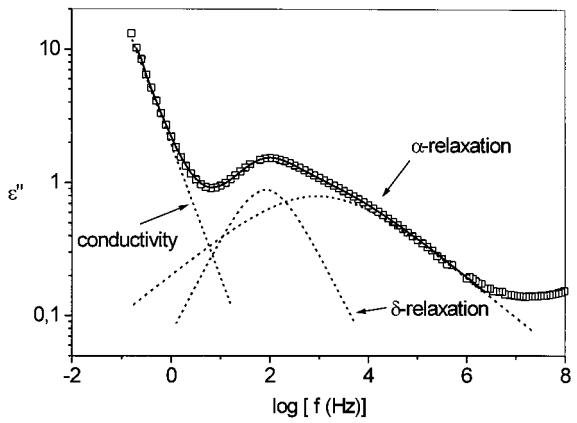

Figure 8. Dielectric loss factor ϵ'' vs frequency for the copolymer **P1** at 78.0 °C. The solid line is the sum of the fit curves, whereas the dashed lines describe the different contributions which parameters are given in Table 3.

be seen that four relaxation processes of dipole polarization are observed. They are designated as δ, α, β, and γ processes in the order of decreasing temperatures. The β and γ processes have low dielectric strength and at the selected frequencies are revealed in the glassy state of the polymer. The stronger δ and α relaxation are active in the LC phase.

To describe quantitatively the dielectric spectra at a fixed temperature, the Fuoss−Kirkwood (FK) function[17] was used. This function was used for description of the dielectric data in many comblike LC polymers[18−21] although it does not have any specific advantages over other symmetric functions:

$$\epsilon''(\omega) = \epsilon''_{max}\ \mathrm{sech}[\beta_{FK}\ \ln(\omega/\omega_{max})] \qquad (1)$$

In this equation, ω_{max} is the relaxation frequency, ϵ''_{max} is the amplitude of the imaginary part of the complex dielectric constant, and β_{FK} is the distribution parameter. In this case the mean relaxation time τ_{max} is $1/\omega_{max}$, and the relaxation strength of the process $\Delta\epsilon = \epsilon_{st} - \epsilon_{\infty}$ (ϵ_{st} and ϵ_{∞} are the dielectric constants at the low- and high-frequency ends of the spectrum) may be expressed by the equation

$$\Delta\epsilon = 2\epsilon''_{max}/\beta_{FK} \qquad (2)$$

The distribution parameter takes the values $0 < \beta_{FK} \leq 1$. In the case of $\beta_{FK} = 1$, the FK function corresponds to a Debye relaxation process.

Figure 7 displays the experimental results of the dielectric loss factor vs the frequency for the **P1** polymer in the LC and the isotropic phases. In this temperature−frequency range a strong overlapping of the α and δ processes is observed. As a result, all curves are very broad, and it was necessary to apply the sum of two FK functions in order to obtain a good description of the spectra. Furthermore, in addition to two FK functions describing the α and δ processes, the following expression was used to take into account the contribution of the conductivity at low frequencies:

$$\epsilon''(\omega) = g/\omega^s \qquad (3)$$

where s and g are fitting parameters. For polymers, the parameter s in most cases has values from 0.5 to 1. The value $s = 1$ is in accordance with an ohmic conduction of the sample. Each FK function involves three independent parameters: ϵ''_{max}, β_{FK}, and ω_{max}. Hence, for a combination of two FK functions and taking into account the conductivity contribution, eight independent parameters are required. During the fit process all parameters are varied. The fit routine gives reproducible results. Figure 8 shows an example for the fit results for the frequency dependence of dielectric losses at 78.0 °C for the polymer P1. The solid line in this figure corresponds to the sum of three contributions shown by dotted lines.

The fitting results of the sum of two FK functions and a term for the conductivity to the experimental $\epsilon''(f)$ data for the **P1** polymer at several temperatures are given in Table 3. It follows from this table that the δ process is characterized by a narrow relaxation time distribution in the LC and the isotropic phases. With increasing the temperature, the spectrum of the δ process gradually becomes narrower. The distribution parameter β_{FK} changes from ∼0.7 in the SmA phase to ∼0.8 in the isotropic melt. Its relaxation strength increases with the temperature, and in the isotropic melt it attains ∼4. The α transition has a wider distribution of relaxation times ($\beta_{FK} \sim 0.3-0.5$), and the relaxation strength decreases considerably with increasing temperature.

As already mentioned, for the polymer **P1** two relaxation processes were also detected in the glassy state. Figure 9 shows frequency dependencies of the dielectric loss factor for **P1** at temperatures below T_g. At temperatures below −50 °C, the absorption maxima of these processes are well separated. To describe the dielectric spectra of **P1** in this temperature range, a combination of two FK functions was also used. The results of fitting are listed in Table 4. From the table it follows that both relaxation have broad distribution of relaxation time: e.g., the distribution parameters β_{FK} at $T = -70$ °C are 0.42 ± 0.01 and 0.27 ± 0.01. The relaxation strength of the γ transition is approximately 4 times higher than that for the β transition.

Figure 10 shows the dependence of the logarithm of the relaxation time on the reciprocal temperature for the processes observed in the **P1** polymer. Both high-frequency relaxations are characterized by linear dependence of the relaxation rate on reciprocal temperature and hence can be described by an Arrhenius equation:

$$\tau = \tau_0 \exp(U/kT) \qquad (4)$$

where τ_0 is the preexponential factor and U is the

Table 3. Fuoss−Kirkwood Fit Parameters for the α and δ Processes in the Copolymer P1

		temp, °C				
process	parameter	72.1	78.0	83.9	92.7	110.4
δ	ϵ_{max}	0.78 ± 0.07	0.92 ± 0.08	1.00 ± 0.09	1.46 ± 0.11	1.72 ± 0.10
	$\Delta\epsilon$	2.3 ± 0.2	2.6 ± 0.3	2.7 ± 0.3	3.9 ± 0.4	4.3 ± 0.4
	τ, s	$(6.9 \pm 0.2) \times 10^{-3}$	$(1.9 \pm 0.1) \times 10^{-3}$	$(5.2 \pm 0.2) \times 10^{-4}$	$(7.8 \pm 0.5) \times 10^{-5}$	$(5.2 \pm 0.2) \times 10^{-6}$
	β_{FK}	0.67 ± 0.03	0.70 ± 0.05	0.74 ± 0.04	0.75 ± 0.5	0.80 ± 0.05
α	ϵ_{max}	0.80 ± 0.05	0.77 ± 0.04	0.81 ± 0.06	0.83 ± 0.07	0.84 ± 0.06
	$\Delta\epsilon$	5.9 ± 0.4	5.1 ± 0.4	4.9 ± 0.4	4.4 ± 0.3	3.7 ± 0.3
	τ, s	$(1.2 \pm 0.1) \times 10^{-3}$	$(1.5 \pm 0.1) \times 10^{-4}$	$(3.9 \pm 0.3) \times 10^{-5}$	$(6.4 \pm 0.5) \times 10^{-6}$	$(5.5 \pm 0.4) \times 10^{-7}$
	β_{FK}	0.27 ± 0.01	0.30 ± 0.01	0.33 ± 0.01	0.38 ± 0.01	0.45 ± 0.03

Table 4. Fuoss−Kirkwood Fit Parameters for the β and γ Processes in the Copolymer P1

		temp, °C				
process	parameter	−60.0	−70.0	−80.0	−90.0	−100.0
β	ϵ_{max}	0.013 ± 0.001	0.013 ± 0.001	0.014 ± 0.001	0.014 ± 0.001	0.015 ± 0.001
	$\Delta\epsilon$	0.056 ± 0.004	0.062 ± 0.005	0.067 ± 0.005	0.074 ± 0.005	0.086 ± 0.006
	τ, s	$(4.7 \pm 0.3) \times 10^{-3}$	$(1.9 \pm 0.1) \times 10^{-2}$	$(9.2 \pm 0.4) \times 10^{-2}$	$(8.7 \pm 0.4) \times 10^{-1}$	6.3 ± 0.5
	β_{FK}	0.43 ± 0.01	0.42 ± 0.01	0.42 ± 0.01	0.38 ± 0.01	0.37 ± 0.01
γ	ϵ_{max}	0.035 ± 0.001	0.033 ± 0.001	0.031 ± 0.001	0.028 ± 0.001	0.026 ± 0.001
	$\Delta\epsilon$	0.25 ± 0.01	0.24 ± 0.01	0.25 ± 0.01	0.24 ± 0.01	0.24 ± 0.01
	τ, s	$(5.2 \pm 0.4) \times 10^{-7}$	$(1.2 \pm 0.1) \times 10^{-6}$	$(3.0 \pm 0.1) \times 10^{-6}$	$(6.9 \pm 0.3) \times 10^{-6}$	$(2.6 \pm 0.1) \times 10^{-5}$
	β_{FK}	0.28 ± 0.01	0.27 ± 0.01	0.25 ± 0.01	0.23 ± 0.01	0.22 ± 0.01

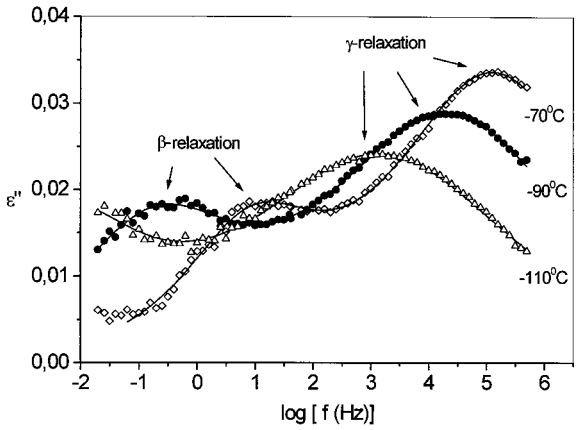

Figure 9. Dielectric loss factor ϵ'' vs frequency for the copolymer **P1** at low temperatures (β and γ relaxation region). The solid lines are the sum of the two FK fit curves.

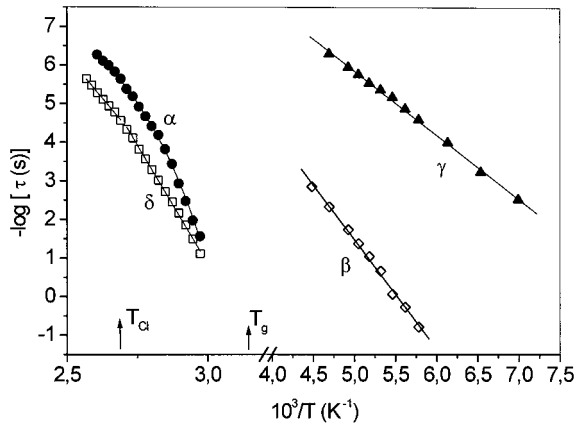

Figure 10. Activation diagram for all relaxation processes in the copolymer **P1**. The errors are smaller than the size of the symbols.

activation energy. The activation energies determined from the slope of these curves are $U_\beta = 54 \pm 2$ kJ/mol for the β process and $U_\gamma = 32 \pm 1$ kJ/mol for the γ process. On the whole, the values for the parameters of the β and the γ transitions are characteristic of dipole relaxation processes of local type, i.e., of reorientation with respect to relatively small portions of the macromolecule.[22]

The dependence of the relaxation rate on the inverse temperature for the δ process can also be adequately described by two straight lines in the LC and in the isotropic phases. An inflection point is observed at the isotropization temperature. In this case the activation energy of the process is greater in the LC phase ($U_\delta = 235 \pm 3$ kJ/mol) as compared to the isotropic melt ($U_\delta = 168 \pm 3$ kJ/mol). Note that a similar behavior of the δ process was observed for many side-chain LC polymers, and in some cases at clearing temperature T_{Cl} a jumpwise increase in relaxation rate is observed followed by linear dependence in the isotropic phase.[23−27]

The α process exhibits a pronounced nonlinear temperature dependence of the relaxation rate in Arrhenius coordinates. Therefore, for its description the phenomenological Vogel−Fulcher equation [28] was used

$$\log f_{max} = \log f_\infty - A/(T - T_v) \qquad (5)$$

where f_{max} is the relaxation frequency; $\log f_\infty$, A, and T_v are the Vogel−Fulcher parameters. The $\log f_\infty$ is the limiting value for the frequency at $T \rightarrow \infty$, T_v is the so-called Vogel temperature which is usually 50 °C lower than T_g, and A has meaning of the activation parameter. The following Vogel−Fulcher parameters were obtained for **P1**: $\log f_\infty = 10.9$, $A = 530$ K, and $T_v = 284$ K. The glass transition temperature was determined at $\tau = 100$ s. The value of $T_g = 50$ °C found in this way exceeds by 8 °C the T_g value found by the DSC method ($T_g = 42$ °C).

3.2.2. Influence of the Annealing Time on the Molecular Dynamics of the Copolymer P1. As already pointed out above, one of the main aims of this work was to study the effect of heat treatment on the molecular dynamics of the LC copolymer. For this purpose samples of **P1** subjected to annealing for 50 (**P1-50**), 100 (**P1-100**), 150 (**P1-150**) and 200 h (**P1-200**) were investigated. The polymers with annealing times of 150 and 200 h exhibited a network structure. For all polymers in the frequency−temperature window used, just as in the case of **P1**, four relaxation processes of dipole polarization were observed.

Table 5. Fuoss−Kirkwood Fit Parameters for the Cooperative Processes in the Copolymer P1 Annealed for Different Times

process	parameters at 89.8 °C	annealing time, h				
		0 (**P1**)	50 (**P1-50**)	100 (**P1-100**)	150 (**P1-150**)	200 (**P1-200**)
δ	ϵ_{max}	1.21 ± 0.1	1.01 ± 0.2	1.06 ± 0.2	1.20 ± 0.4	1.20 ± 0.05
	τ, s	(1.5 ± 0.1) × 10^{-4}	(8.3 ± 0.3) × 10^{-4}	(3.1 ± 0.2) × 10^{-3}	(1.7 ± 0.3) × 10^{-2}	(7.2 ± 1.3) × 10^{-2}
	β_{FK}	0.75 ± 0.04	0.64 ± 0.04	0.55 ± 0.03	0.50 ± 0.07	0.45 ± 0.09
α	ϵ_{max}	0.85 ± 0.08	0.65 ± 0.10	0.43 ± 0.09	0.35 ± 0.10	0.24 ± 0.09
	τ, s	(1.2 ± 0.1) × 10^{-5}	(1.2 ± 0.2) × 10^{-4}	(4.2 ± 0.7) × 10^{-4}	(2.1 ± 0.8) × 10^{-3}	(1.1 ± 0.6) × 10^{-2}
	β_{FK}	0.37 ± 0.01	0.29 ± 0.01	0.25 ± 0.01	0.18 ± 0.4	0.15 ± 0.03

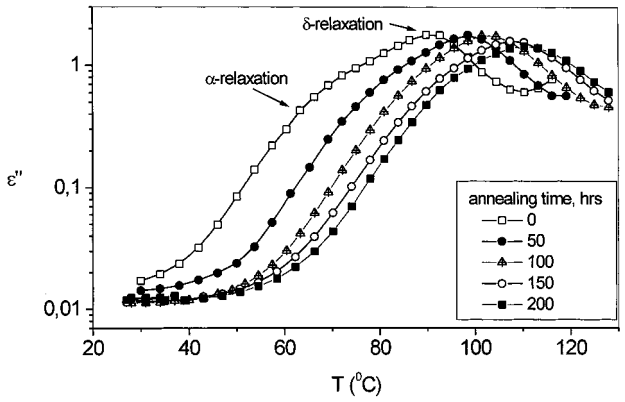

Figure 11. Dielectric loss factor ϵ'' at 1 kHz vs the temperature for the copolymer **P1** annealed at 130 °C for different times.

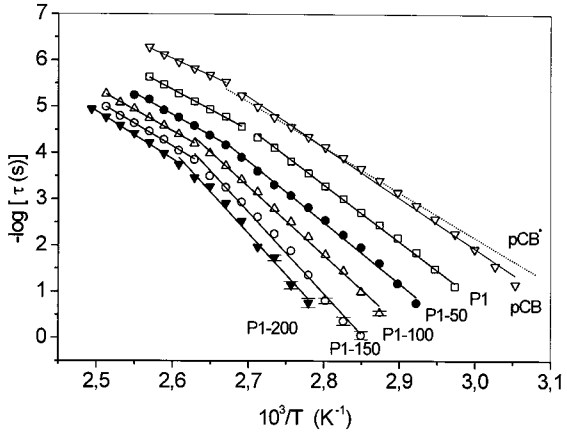

Figure 12. Activation diagram for the δ process in the copolymer **P1** annealed for different time and in LC homopolymer **pCB** (**pCB***: reported in ref 20). Lines are the fits of the Arrhenius equation to the data.

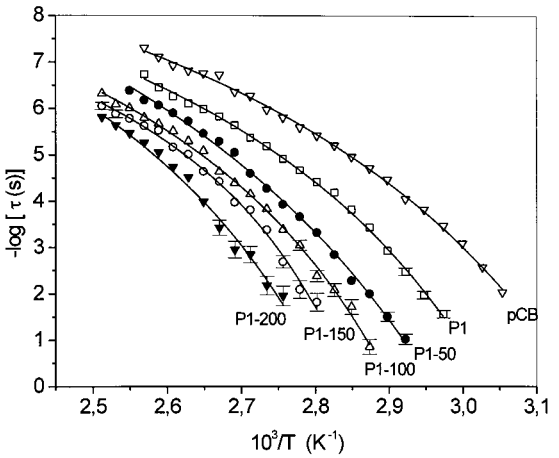

Figure 13. Activation diagram for the α process in the copolymer **P1** annealed for different time and in LC homopolymer **pCB**. Lines are the fits of the Vogel−Fulcher equation to the data.

Figure 11 shows the temperature dependence of ϵ'' at a frequency of 1 kHz for samples with different annealing times. It can be seen that after annealing the main dispersion maximum appearing in the LC state is significantly displaced toward higher temperatures. The bimodal character of the dielectric absorption (existence of δ and α processes) is distinctly observed for the samples with an annealing time up to 100 h, i.e., until a network is formed. For samples **P1-150** and **P1-200**, the α process is represented by a poorly resolved low-temperature shoulder on the experimental curves. However, we believe that with the formation of a network structure this process does not disappear but becomes broader as can be seen for dielectric spectra of segmental motion in polymer networks.[29−31] Therefore, it is more difficult to distinguish this process for samples **P1-150** and **P1-200**. For the above reasons, to describe quantitatively the dielectric spectra of samples with different annealing times in the LC and the isotropic phases, a combination of two FK functions was used, and the conductivity contribution was also taken into account.

The fitting results are summed up in Table 5, and Figures 12 and 13 display the dependence of the logarithm of the relaxation time on the reciprocal temperature for the δ and α processes, respectively. The straight lines describe adequately the temperature dependence of the relaxation rate of the δ process in the smectic and the isotropic phase. For each polymer the inflection point is observed at the clearing temperature. With increasing an annealing time, the relaxation process becomes greatly hindered. The overall change in relaxation time at 89.8 °C is more than 2 orders of magnitude. The activation energy increases simultaneously both in the liquid crystalline and in the isotropic phases. It should be noted that in the LC state the activation energy is much larger than that in the isotropic melt (see also Table 6).

A strong dependence of the relaxation rate on the annealing time was also detected for the α process (Figure 13). The Vogel−Fulcher parameters for the α process are given in Table 6. For all samples, higher T_g value were determined by the dielectric method than by the DSC method.

No significant effect of the annealing on the parameters of the low-temperature β and γ processes was found (Table 7). In general, the corresponding dependencies for the γ process for all samples studied lie about a straight line with activation energy U_γ = 32 kJ/mol and $\tau_\gamma \sim 7 \times 10^{-6}$ s (at −90 °C). Polymers **P1**, **P1-50**, and **P1-100** have also identical parameters for the β process: U_β = 54 kJ/mol and $\tau_\beta \sim 0.9$ s (at −90 °C). However, for networks **P1-150** and **P1-200**, the activation energy of the β process increases slightly and is 56

Table 6. Influence of the Annealing Time on the δ and α Relaxation Parameters. Constants of the Fit to Eq 4 for the δ and to Eq 5 for the α Processes

		annealing time, h				
process	parameter[a]	0 (**P1**)	50 (**P1-50**)	100 (**P1-100**)	150 (**P1-150**)	200 (**P1-200**)
δ	U, kJ/mol LC/I	235/168	252/174	282/174	337/186	341/196
	log τ_0 LC/I	−37.8/−28	−39.5/−28.6	−43.4/−28.2	−50.4/29.5	−50.5/−30.8
α	log(f_∞)	10.9 ± 0.4	12.8 ± 0.8	10.6 ± 0.5	9.3 ± 0.6	11.4 ± 1.71
	A	530 ± 55	823 ± 95	487 ± 53	309 ± 59	561 ± 140
	T_v, K	284 ± 3	277 ± 6	301 ± 4	320 ± 5	308 ± 15
	T_g, °C[b]	50	57	64	72	74

[a] LC is the liquid crystalline state; I is the isotropic melt. [b] Determined from Vogel−Fulcher dependence at $\tau = 100$ s.

Table 7. Influence of the Annealing Time on the β and γ Relaxation Parameters. Constants of the Fit to Eq 4

		annealing time, h				
process	parameter	0 (**P1**)	50 (**P1-50**)	100 (**P1-100**)	150 (**P1-150**)	200 (**P1-200**)
γ	U, kJ/mol	32 ± 1	32 ± 1	32 ± 1	32 ± 1	32 ± 1
	τ, s at −90 °C	(6.9 ± 0.3) × 10^{-6}	(6.6 ± 0.3) × 10^{-6}	(7.1 ± 0.4) × 10^{-6}	(6.7 ± 0.3) × 10^{-6}	(6.9 ± 0.4) × 10^{-6}
	log τ_0	−14.2 ± 0.1	−14.1 ± 0.1	−14.1 ± 0.1	−14.4 ± 0.1	−14.4 ± 0.1
β	U, kJ/mol	54 ± 1	54 ± 1	54 ± 1	56 ± 1	58 ± 1
	τ, s at −90 °C	0.87 ± 0.05	0.80 ± 0.05	0.93 ± 0.06	0.95 ± 0.05	1.05 ±0.08
	log τ_0	−15.3 ± 0.3	−15.0 ± 0.3	−15.7 ± 0.3	−16.0 ± 0.4	−15.9 ± 0.5

and 58 kJ/mol, respectively. The relaxation times at $t = -90$ °C are 0.95 and 1.05 s, respectively. The relaxation strength of the β and γ processes does not change with the annealing.

3.2.3. Mechanism of Motions. First of all, it is very interesting to compare the dielectric behavior of the functionalized LC copolymer **P1** and related LC homopolymer **pCB** in order to understand the mechanism of the molecular motions in both systems. Unfortunately, in the literature only the parameters of the cooperative motions for the **pCB** polymer are avaible.[20,32] For this reason we investigated additionally the local dynamics in the **pCB** polymer ($M_n = 3.39 \times 10^3$, $M_w = 5.59 \times 10^3$, *glass 43 N 101 I*) at temperatures down to −150 °C. The parameters of the cooperative motions were also obtained. Our study shows that the dielectric spectra of the **pCB** polymer and of the copolymer **P1** have several common features. The **pCB** polymer also exhibits four relaxation processes in the investigated temperature−frequency window. In the liquid crystalline and the isotropic phases, intensive δ and α transitions are observed, and in the glassy state the dielectrically less active β and γ processes are also detected. Moreover, it is confirmed that for these systems the parameters of both local processes virtually coincide and, hence, have an identical mechanism. However, the values of the relaxation time of the cooperative motions exhibit considerable differences, as it is seen from Figures 12 and 13. In the functionalized **P1** copolymer both relaxation processes are considerably hindered as compared to those in the **pCB** polymer. This is due to the formation of eight-membered pseudocyclic rings, which cause a loss of kinetic flexibility of the main chain.[5] Hence, one can conclude that the dynamic conditions in the **pCB** polymer are different than those in the LC copolymer **P1** due to difference in the flexibility of the main chains. However, we emphasize the fact that the nature of the dielectrically active local and cooperative motions in both polymers remains the same.

In some polymer systems the presence of the hydrogen bonds can lead to a considerable change in the relaxation mechanism. This is an additional sense to compare the dielectric behavior of the **pCB** polymer and the functionalized LC polymer **P1.** For example, the appearance of two α processes (α and α* relaxation) is observed for polybutadienes modified by a small amount of 4-phenyl-1,2,4-triazoline-3,5-dione.[33,34] The α* relaxation is assigned to the local complex dynamics resulting from the dissociation and formation of dimeric contacts between the triazoline fragments.

3.2.3.1. Local Processes. The local processes of dipole polarization relaxation reflect the mobility of kinetic units with a relatively small volume. The parameters of these processes mainly depend on the nearest environment along the chain (intramolecular barrier of internal rotation) and usually depend only slightly on the supramolecular polymer structure. In other words, they have a pronounced noncooperative character.[22] Chemical changes in the polymer, which do not involve directly the mobile fragment, do not affect its mobility, either. Hence, in samples containing fragments with the polar groups and the same structure, the relaxation rates of dipole polarization of the corresponding local transitions are approximately equal. This is an important point when dielectric spectra of different polymers are compared.

***γ* Relaxation.** As already mentioned, the γ process is observed in the glassy state, and its parameters do not depend on the annealing. The activation energy of the γ relaxation was $U_\gamma = 32$ kJ/mol at relaxation time $\tau_\gamma \sim 7 \times 10^{-6}$ s (at −90 °C). In side-chain LC polymers this process is usually considered to depend on the spacer mobility. A study of the dynamic mechanical losses for different polymers shows that it is necessary to incorporate a sequence of at least four methylene units into the polymer chain in order to obtain its own characteristic relaxation transition at a frequency of 10 Hz at ∼−120 °C.[35] Since the methylene spacer fragment is nonpolar, its motion can be dielectrically active if some adjacent polar group takes part in it.[36]

The γ process was detected for most side-chain LC polymers.[21,37−40] It should be pointed out that in a LC poly(acrylate) with a short spacer consisting only of two methylene groups this transition is not observed.[39] Hence, one can assume with confidence that the γ process is due to the mobility of the alkyl fragment with adjacent oxygen atoms. In the process of annealing the appearing intra- and intermolecular anhydrides do not directly affect the spacer. Therefore, the parameters of its local motion do not change.

***β* Relaxation.** The existence of the β dielectric transition is caused by the rotation of the mesogenic side

group about its long axis. This process has been detected in the glassy state for many side-chain LC polymers.[21,37−43] The appearance of the β dielectric process in **P1** should be related to the presence of an ether bond between the cyanobiphenyl mesogenic group and the spacer. The ether bond has a component of dipole moment directed normally to the long axis of the mesogenic group. Although the nitrile group has a high dipole moment (4.2 D),[44] it does not provide any contribution to the dielectric losses because its dipole moment is directed coaxially to the long axis of the mesogenic group. At high frequencies of 10^7-10^9 Hz, the β process is also active in the LC and the isotropic phases.[41] As a whole, the relaxation time and the activation energy of a given motion are defined basically by the sizes of the mesogenic fragment and depend only slightly on the type of the mesomorphic phase and the spacer length, except for the case of a short spacer consisting of two methylene groups, where an effective decoupling between the mesogen and the main chain motions is not reached.[41] When the spacer contains more than six methylene groups, the parameters of the β relaxation practically do not vary. In contrast to the γ process, the parameters of the β relaxation can be sensitive to some morphological features of the polymer because the relatively bulky phenyl rings participating in this motion are subjected to strong steric interactions with the nearest environment. Hence, to some extent this process may be regarded as cooperative.[38,43]

It was shown that during annealing the activation energy of this motion increases slightly: from 54 kJ/mol for **P1** to 58 kJ/mol for **P1-200**. At the same time the relaxation strength of the β process does not depend on annealing. Only a slight broadening of the relaxation spectrum was observed. The distribution parameter β_{FK} at −90 °C decreases from 0.38 ± 0.01 (**P1**) to 0.33 ± 0.01 (**P1-200**). This indicates a certain increase in the microheterogeneity of the system. However, on the whole changes in the parameters of the β relaxation during annealing are insignificant.

Consequently, the parameters of the γ and β processes essentially do not change when the system transforms from a linear to a network. The fact that the parameters of both processes do not depend on the annealing confirms the above conclusions about the character of the intra- and intermolecular anhydride rings. The formation of the anhydride structures is a result from macromolecular transformations of the acrylic acid groups. At the same time mesogenic groups do not take part in the anhydride formation.

3.2.3.2. Cooperative Processes. Cooperative relaxation processes reflect the motion of the relatively long parts of the macromolecule. The parameters of these motions are most sensitive to morphological and chemical features of the polymer. For a large number of side-chain LC polymers two cooperative relaxation processes were detected near the glass transition temperature.

Here it is appropriate to mention that the nature of these relaxations at a molecular level is a controversial subject. Up to the present there is no single view on the mechanisms of the δ and α processes. Different models for description of these processes are proposed.[23,24,45,46] The most extensively discussed model for the low-frequency δ relaxation assumes that it is caused by cooperative rotation of the side groups. The large relaxation strength and its dependence on the longitudinal component of the side groups dipole moment confirm this model. Moreover, the low-frequency relaxation has a narrow absorption curve. In contrast, the high-frequency α relaxation is characterized by a very broad maximum of dielectric absorption. The temperature dependence of the α relaxation rate is essentially nonlinear in the Arrhenius coordinates and is analogous to that of the dynamic glass transition in amorphous polymers. In most cases the appearance of this process coincides with the glass transition temperature of the polymer, which is also a formal basis for referring it to segmental motion.

On the other hand, for oriented polymers it has been shown that the relaxation strength of the α process strictly depends on the transverse constituent of the dipole moment of the side group. It is also assumed that the α relaxation can be described by a combined molecular motion consisting of the segmental motion of the main chain and the rotation of the side group around the short axis. It is quite evident that, in the framework of the traditional dielectric measurements, it is not possible to separate the contributions of these motions because they are characterized by close relaxation times. It is natural that, depending on the chemical structure of the polymer, the contribution of each of the above motions to the combined α process will be different. Thus, for comblike LC polymers with a siloxane main chain that does not have a strong dipole moment, the α process is dominated by the contribution of the transverse component of the dipole moment of the side group.[24] However, for combined main chain−side chain LC polymers with a backbone containing strong polar groups, a typical dynamic glass transition process is observed.[42]

Recently interesting results have been obtained by another dielectric related method—thermally stimulated discharge currents (TSDC).[47−49] This method has a high resolution. Therefore, for systems with pronounced $\mu_\perp$ and $\mu_\parallel$ components of the side group dipole moment, it was possible to separate the contribution of the main chain to the polarization of the segmental motion from those of the corresponding components of the side chain. For these systems, three corresponding relaxation processes of dipole polarization were observed in the glass transition region. It is interesting that for polymers containing a cyanobiphenyl mesogenic fragment, i.e., having predominantly only $\mu_\parallel$ for the side chain, only one polarization process in addition to the glass transition was observed by the TSDC method. This process may be related to the δ transition of the dipole polarization relaxation. This fact implies that for these systems the α relaxation observed by the dielectric method corresponds to a greater extent to the dynamic glass transition process.

The acid fragment of the **P1** copolymer has a strong dipole moment, whereas $\mu_\perp$ of the mesogenic side group is determined mainly by the adjacent ether group with a dipole moment of 1.22 D. Hence, it should be expected that in **P1** the segmental motion of the main chain provides the greatest contribution to the combined α process. This fact in particular can explain the high value of the relaxation strength of this process, $\Delta\epsilon_\alpha = 5.1 \pm 0.5$ in the LC phase at 78 °C, which considerably exceeds the value for the δ relaxation, $\Delta\epsilon_\delta = 2.6 \pm 0.3$. For the related LC polymer **pCB** at the same temperature we have obtained $\Delta\epsilon_\alpha = 3.39 \pm 0.4$ and $\Delta\epsilon_\delta = 3.08 \pm 0.3$, i.e., $\Delta\epsilon_\delta \cong \Delta\epsilon_\alpha$.

As has been established by IR spectroscopy, the acid fragment of the **P1** copolymer is characterized by formation of intramolecular hydrogen bonds between the free carboxyl groups,[5] which leads to formation of stable eight-membered alicyclic rings (Figure 2a). As a result, the rigidity of the main polymer chain increases. This is the principal reason for the differences in the dynamic characteristics of the δ and α processes in the functionalized copolymer **P1** and in the **pCB** polymer because it has been experimentally established that the temperature position of both cooperative processes is strictly controlled by the main chain rigidity.[25,50,51] For example, the relaxation time of the δ process in LC poly(methacrylate) is 10^3 times longer than that in poly(acrylate) having an identical spacer and mesogenic groups.[25] As the main chain becomes more rigid and, hence, T_g also increases, in the series methylsiloxane, acrylate, methacrylate and chloroacrylate the δ peak gradually becomes broader and is displaced toward low frequencies. The activation energy of this transition in this polymer series also increases.[50,51]

A similar behavior of the δ relaxation was found in **P1** during heat treatment: the parameter β_{FK} decreases from 0.75 (at 89.8 °C) for **P1** to 0.55 for **P1-100**, and the relaxation time increases from $(1.5 \pm 0.1) \times 10^{-4}$ to $(3.1 \pm 0.2) \times 10^{-3}$ s. Further increase in the annealing time (150, 200 h) leads to a network formation, and the width of the δ relaxation spectrum increases additionally to $\beta_{FK} = 0.45$ for **P1-200**. The relaxation time and the activation energy for networks also depend on the heat treatment time (Table 5).

It should be noted that the formation of a weakly cross-linked network has only a slight effect on the parameters of the cooperative δ and α processes[32] and the phase transitions.[52,53] However, to the best of our knowledge there are no papers on dielectric relaxation in densely cross-linked LC polymers. It should be assumed that with increasing the cross-linking density the segmental motion spectrum should become broader and is displaced toward the low-frequency region as it has been shown for many common polymer networks.[29−31] As a result, the relaxation time of both cooperative processes should also increase.

In fact, for network samples **P1-150** and **P1-200** an additional increase in τ was observed for the δ and α transitions with simultaneous broadening of the spectra for both processes (samples **P1-150** and **P1-200** are compared in Table 5). As pointed out in the first part of this work, the maximum contribution to the increase of the transition temperatures caused by six-membered intramolecular rings is observed for annealing times up to 50 h. Further heat treatment of the polymer leads only to a slight increase in the intensity of the intramolecular anhydride bands [$\nu_{C=O}$]. For annealing times of 150−200 h, the integral intensity of the D_{1762}/D_{1748} ratio does not change within the experimental error of the method (5%). In other words, for annealing times of 150−200 h, the formation of new intramolecular anhydride rings does not take place. Therefore, it may be reasonable to suggest that the experimentally observed additional increase in the relaxation time for the δ and α transitions in the polymers **P1-150** and **P1-200** is caused by the formation of intermolecular anhydrides, which results in increasing cross-link density of the polymer network.

4. Conclusions

The present work investigates the anhydrization of a side chain functionalized LC copolymer containing acrylic acid groups. It was shown that the thermal treatment of the samples at 130 °C for 5−200 h is accompanied by the formation of intra- and intermolecular anhydrides as well as network structures. Polymer products, obtained as a result of the heat treatment, show an increase of the glass transition and the clearing temperatures of the LC polymer **P1**. At the same time the formation of six-membered intramolecular rings between the neighboring acrylic acid units exerts the greatest effect on the phase behavior of the polymer. The reorientation dynamics of LC copolymers was studied by dielectric spectroscopy. The local mobility of the side group including the spacer motion (γ-relaxation) and the rotation of the mesogenic group around the long axis (β-relaxation) does not depend on the annealing time because the side group does not participate in the formation of anhydride rings. Hence, the local dynamics of the side group cannot change after the annealing. However, a significant (by more than 2 orders of magnitude) decrease in the relaxation rate of the cooperative δ and α processes was observed. The α process is assigned to micro-Brownian motion of the main chain, and therefore its relaxation rate strongly decreases due to a gradual increase in the backbone rigidity during the annealing. At the same time the relaxation rate of the δ process (motion of the side group as a whole) also decreases. This is a clear evidence of a very strong dynamical coupling between the mesogenic fragment and the backbone chain.

Acknowledgment. This research was supported by INTAS (Ref. Nr. 97-1936) and personally (E. B. Barmatov) by Alexander von Humboldt Foundation (Germany).

References and Notes

(1) Kato, T.; Frechet, M. J. *Macromol. Symp.* **1995**, *98*, 311.
(2) Kato, T. *Hydrogen-Bonded Systems in Handbook of Liquid Crystals, IIB*; Wiley-VCH: Weinheim, 1997; p 969.
(3) Paleos, C. M.; Tsiourvas, D. *Angew. Chem., Int. Ed. Engl.* **1995**, *34*, 1696.
(4) Bazuin, C. G. *Mechanical and Termophysical Properties of Polymer Liquid Crystals*; Chapman & Hall: London, 1998; Vol. 3, p 59.
(5) Barmatov, E. B.; Pebalk, D. A.; Barmatova, M. V.; Shibaev, V. P. *Liq. Cryst.* **1997**, *23*, 447.
(6) Barmatov, E. B.; Barmatova, M. V.; Grokhovskaya, T. E.; Shibaev, V. P. *Polym. Sci.* **1998**, *40*, 295.
(7) Shibaev, V. P.; Barmatov, E. B.; Barmatova, M. V. *Colloid Polym. Sci.* **1998**, *276*, 662.
(8) Barmatov, E.; Barmatova, M.; Kremer, F.; Shibaev, V. *Macromol. Chem. Phys.* **2000**, *201*, 2597.
(9) Barmatov, E. B.; Bobrovsky, A. Yu.; Barmatova, M. V.; Shibaev,V. P. *Polym. Sci.* **1998**, *40*, 1769.
(10) Barmatov, E. B.; Bobrovsky, A. Yu.; Barmatova, M. V.; Shibaev, V. P. *Liq. Cryst.* **1999**, *26*, 581.
(11) Barmatov, E. B.; Bobrovsky, A. Yu.; Pebalk, D. A.; Barmatova, M. V.; Shibaev, V. P. *J. Polym. Sci., Part A: Polym. Chem.* **1999**, *37*, 3215.
(12) Barmatov, E.; Filippov, A.; Andreeva, L.; Barmatova, M.; Kremer, F.; Shibaev, V. *Macromol. Rapid Commun.* **1999**, *20*, 521.
(13) Filippov, A. P.; Andreeva, L. N.; Barmatov, E. B.; Barmatova, M. V.; Grande, S.; Kremer, F.; Shibaev, V. P. *Polym. Sci.* **2000**, *42*, 329.
(14) Plate, N. A.; Litmanovich, A. D.; Noah, O. V. *Macromolecular Reaction*; John Wiley & Sons: Guildford, 1995.
(15) Lezov, A. V.; Rjumtsev, E. I.; Polushin, S. G.; Melnikov, A. B.; Tarasenko, K. N.; Polushina, G. E.; Barmatov, E. B.; Schaumburg, K.; Shibaev, V. P. *Liq. Cryst.*, in press.

(16) Novotna, E.; Kostromin, S. G.; Kresse, H. *Liq. Cryst.* **1995**, *18*, 73.
(17) Fuoss, R. M.; Kirkwood, J. G. *J. Am. Chem. Soc.* **1941**, *63*, 385.
(18) Attard, G. S.; Williams, G. *Liq. Cryst.* **1986**, *1*, 253.
(19) Bormuth, F. J.; Haase, W. *Liq. Cryst.* **1988**, *3*, 881.
(20) Bormuth, F. J.; Biradar, A. M.; Quotschalla, U.; Haase, W. *Liq. Cryst.* **1989**, *5*, 1549.
(21) Zhong, Z. Z.; Schuele, D. E.; Gordon, W. L. *Liq. Cryst.* **1994**, *17*, 199.
(22) Starkweather, Jr., H. W. *Macromolecules* **1988**, *21*, 1798.
(23) Haase, W.; Pranoto, H.; Bormuth, F. J. *Ber. Bunsen-Ges. Phys. Chem.* **1985**, *89*, 1229.
(24) Attard, G. S.; Williams, G.; Gray, G. W.; Lacey, D.; Gemmel, P. A. *Polymer* **1986**, *27*, 185.
(25) Kresse, H.; Kostromin, S.; Shibaev, V. *Makromol. Chem., Rapid Commun.* **1982**, *3*, 509.
(26) Nikonorova, N. A.; Borisova, T. I. *Polym. Sci.* **1993**, *35*, 30.
(27) Attard, G. S.; Williams, G.; Fawcett, A. H. *Polymer* **1990**, *31*, 928.
(28) Vogel, K. *Phys. Z.* **1921**, *22*, 645.
(29) Glatz-Reichenbach, J. K. W.; Sorriero, L. J.; Fitzgerald, J. J. *Macromolecules* **1994**, *27*, 1338.
(30) Roland, C. M. *Macromolecules* **1994**, *27*, 4242.
(31) Andjelic, S.; Mijovic, J. *Macromolecules* **1998**, *31*, 8463.
(32) Nikonorova, N. A.; Barmatov, E. B.; Borisova, T. I.; Shibaev, V. P. *Polym. Sci.* **1997**, *39*, 404.
(33) Müller, M.; Kremer, F.; Stadler, R.; Fischer, E. W.; Seidel, U. *Colloid Polym. Sci.* **1995**, *273*, 38.
(34) Müller, M.; Stadler, R.; Kremer, F.; Williams, G. *Macromolecules* **1995**, *28*, 6942.
(35) Willbourn, A. H. *Trans. Faraday Soc.* **1958**, *54*, 717.
(36) Wetton, R. E.; Williams, G. *Trans. Faraday Soc.* **1965**, *61*, 2132.
(37) Gedde, U. W.; Liu, F.; Hult, A.; Sahlen, F.; Boyd, R. H. *Polymer* **1994**, *35*, 2056.
(38) Hellermark, C.; Gedde, U. W.; Hult, A.; Boeffel, C.; Boyd, R. H.; Liu, F. *Macromolecules* **1998**, *31*, 4531.
(39) Zentel, R.; Strobl, G.; Ringsdorf, H. *Macromolecules* **1985**, *18*, 960.
(40) Borisova, T. I.; Nikonorova, N. A. *Macromol. Chem. Phys.* **1998**, *199*, 2147.
(41) Schönfeld, A.; Kremer, F.; Hofmann, A.; Kühnpast, K.; Springer, J.; Scherowsky, G. *Makromol. Chem.* **1993**, *194*, 1149.
(42) Kremer, F.; Vallerien, S. U.; Zentel, R.; Kapitza, H. *Macromolecules* **1989**, *22*, 4040.
(43) Schönhals, A.; Wolff, D.; Springer, J. *Macromolecules* **1995**, *28*, 6254.
(44) Klinbiel, R. T.; Genova, D. J.; Criswell, T. R.; Meter, J. P. *J. Am. Chem. Soc.* **1974**, 7651.
(45) Williams, G. *Polymer* **1994**, *35*, 1915.
(46) Schönhals, A.; Wolff, D.; Springer, J. *Macromolecules* **1998**, *31*, 9019.
(47) Mano, J. F.; Correia, N. T.; Moura Ramos, J. J. *Polymer* **1994**, *35*, 3561.
(48) Mano, J. F.; Moura Ramos, J. J.; Anabela, F.; Williams, G. *Polymer* **1994**, *35*, 5170.
(49) Mano, J. F.; Correia, N. T.; Williams, G. *Liq. Cryst.* **1996**, *20*, 201.
(50) Bormuth, F. J.; Haase, W. *Mol. Cryst. Liq. Cryst.* **1987**, *153*, 207.
(51) Haase, W.; Bormuth, F. J.; Pfeiffer, M.; Jakob, E. *Ber. Bunsen-Ges. Phys. Chem.* **1991**, *95*, 1050.
(52) Zentel, R.; Reckert, G. *Makromol. Chem.* **1986**, *187*, 1915.
(53) Zentel, R.; Reckert, G.; Bualek, S.; Kapitza, H. *Makromol. Chem.* **1989**, *190*, 2869.

MA0018401